Characteristic Function of Fundamental and Harmonic Active Power in Digital Measurements Under Nonsinusoidal Conditions

Diego Bellan

Department of Electronics, Information and Bioengineering – Politecnico di Milano, Milan, Italy.

Abstract – *This work provides the analytical derivation of the characteristic function of noisy digital measurements of fundamental and harmonic active power in electrical systems. Knowledge of the characteristic function, in fact, allows a complete statistical description of the measured active power since both the probability density function and the distribution function can be readily derived. Moreover, from the characteristic function all the statistical moments can be evaluated, whereas in the existing literature only the first- and second-order moments of the fundamental component were provided. More specifically, it is well known that voltage and current waveforms in electrical systems under non-sinusoidal conditions are digitized through analog-to-digital conversion and transformed into the frequency domain. Each waveform spectral line is processed to evaluate active power at the corresponding frequency. Since spectral lines are affected by additive noise the measured active power can be properly treated as a random variable. In particular, harmonic active power is more sensitive to additive noise since it is given by low-magnitude spectral lines .In the paper, the probability density function corresponding to the derived characteristic function is validated through numerical simulation of the whole measurement process and the impact of waveform and sampling parameters is investigated.*

Keywords: *Additive Noise Propagation, Discrete Fourier Transform, Power Measurement, Power Quality, Probabilistic Techniques*

Nomenclature

Δf	Frequency resolution of DFT
$\Phi_A(\omega)$	Characteristic function of the random variable A
φ_h	Phase of the h-th frequency component of voltage
μ_A	Statistical mean value of the random variable A
σ_I^2, σ_V^2	Variance of real and imaginary parts of current/voltage DFT coefficients
$\sigma_{n_i}^2$	Variance of current additive noise
$\sigma_{n_v}^2$	Variance of voltage additive noise
ϑ_h	Phase of the h-th frequency component of current
A/D	Analog-to-digital
DFT	Discrete Fourier transform
ENBW	Equivalent noise bandwidth
$f_A(\cdot)$	Probability density function of the random variable A
FFT	Fast Fourier transform
f_h	Frequency of the h-th sine wave component
f_S	Sampling frequency
I_h	Rms amplitude of the h-th component of current
$\hat{I}_h$	DFT estimate of I_h
$M_A(s)$	Moment-generating function of the random variable A
m_n	n-th statistical moment
N	Number of sine waves in voltage/current waveform
N_H	Number of harmonics
n_i, n_v	Additive noise in current/voltage waveforms
N_S	Number of samples
NPSG	Normalized peak signal gain
P_1	Fundamental active power
P_h	Active power related to the h-th frequency component
$\hat{P}_h$	DFT estimate of P_h
P_H	Harmonic active power
PDF	Probability density function
rms	Root mean square
RV	Random variable
SNR	Signal-to-noise ratio
V_h	Rms amplitude of the h-th component of voltage
$\hat{V}_h$	DFT estimate of V_h
$w[\cdot]$	Time window
$\Im_A$	Imaginary part of A
$\Re_A$	Real part of A

I. Introduction

Nowadays, power measurement in electrical systems can be effectively performed by means of digital techniques [1]. Analog-to-digital conversion of voltage and current waveforms, in fact, can be easily and accurately carried out. When only the measurement of

This is the accepted version of Bellan D., "Characteristic function of fundamental and harmonic active power in digital measurements under nonsinusoidal conditions" (International Review of Electrical Engineering, 2015, 10:4, 520-527).
The final publication is available at: http://dx.doi.org/10.15866/iree.v10i4.7052

the average power is required, the digital processing consists simply in the evaluation of the time-domain mean value of the product of the sampled waveforms [2], [3]. In modern electrical power systems, however, the widespread use of non-linear loads results in voltage and current waveforms rich in harmonics and inter-harmonic contents [4]-[6]. Therefore, as far as power is concerned, the resulting non-sinusoidal condition includes a flux of active power at each frequency component of the waveforms spectra [7], [8]. A detailed power-quality analysis requires the measurement of the significant power components associated with the frequency contents of voltage and current waveforms [7], [9], [10].

Thus, each waveform is usually transformed into the frequency domain through the discrete Fourier transform (DFT), and the power components are evaluated by processing the relevant spectral lines [6], [11]. Additive noise coming from the electrical system and from instrumentation [12]-[15] affects the spectral lines amplitude and phase, and therefore each power component must be properly treated as a random variable. Since the harmonic/inter-harmonic spectral lines are much lower in magnitude than the fundamental component (i.e., the component at 50 or 60 Hz in most of power systems), a significant influence of additive noiseis expected on the estimation of the related power components [7]. Thus, the main objective of this work consists in the complete statistical characterization of both the fundamental active power and the harmonic active power related to the contribution of spectral lines different from the fundamental. In the existing literature only the fundamental active power has been investigated by deriving its mean value and variance [2], [11], [15].

In this paper the characteristic function of each component of the active power is derived in closed form.

This allows a complete characterization in terms of probability density function (PDF), distribution function, and all the statistical moments for both the fundamental and the harmonic active power.

The paper is organized as follows. In Section II the background and the main definitions are provided.

In Section III the characteristic function of measured active power is derived in closed form. In Section IV the mean value and the variance are derived from the characteristic function derived in Section III. In Section V the analytical expression of the PDF is derived in integral form.

The analytical results are validated in Section VI through numerical simulation of the whole measurement process. Finally, conclusions are drawn in Section VII.

II. Background and Problem Statement

Power measurements under non-sinusoidal conditions can be effectively performed by resorting to digital instrumentation based on A/D conversion of voltage and current waveforms, and time-to-frequency transformation through the DFT algorithm (by means of the efficient fast Fourier transform (FFT) algorithm) [1], [6], [11], [15].

Thus, active power at each frequency of interest can be readily evaluated by processing the relevant spectral lines. When low-amplitude spectral lines are involved (e.g., when power related to harmonic components must be evaluated), an important source of uncertainty is additive noise. Indeed, voltage/current waveforms are always affected by additive noise which propagates through A/D conversion and DFT transformation, yielding noisy spectral lines.

It is expected that the impact of additive noise is larger as the amplitude of the involved harmonic spectral lines decreases. Therefore, the resulting power evaluations should be properly characterized in statistical terms by treating each power estimate as a random variable (RV).

More specifically, the time-domain voltage/current waveforms are modelled as a sum of the mean value, N sine waves, and additive zero-mean independent noise:

$$v(t) = V_0 + \sqrt{2}\sum_{h=1}^{N} V_h \cos\left(2\pi f_h t + \varphi_h\right) + n_v(t) \quad (1)$$

$$i(t) = I_0 + \sqrt{2}\sum_{h=1}^{N} I_h \cos\left(2\pi f_h t + \vartheta_h\right) + n_i(t) \quad (2)$$

where additive noise takes into account both the noise from the electrical power system and the noise superimposed to the waveforms by the instrumentation.

The fundamental and the harmonic active power are defined as [7]

$$P_1 = V_1 I_1 cos(\varphi_1 - \theta_1) \quad (3)$$

$$P_H = \sum_{h\neq 1} V_h I_h cos(\varphi_h - \theta_h) = \sum_{h\neq 1} P_h \quad (4)$$

After A/D conversion of (1)-(2) with sampling frequency f_s, and weighting time-window $w[\cdot]$ against spectral leakage (N_S samples in length) [16]-[18], the DFT transform provides the estimates of the complex Fourier coefficients:

$$\hat{V}_n = \frac{\sqrt{2}}{N_S NPSG}\sum_{k=0}^{N_S-1} v[k]w[k]exp(-j2\pi kn/N_S) \quad (5)$$

$$\hat{I}_n = \frac{\sqrt{2}}{N_S NPSG}\sum_{k=0}^{N_S-1} i[k]w[k]exp(-j2\pi kn/N_S) \quad (6)$$

where $w[k]$ is the selected time window characterized by the related Normalized Peak Signal Gain NPSG (see Table I where three examples of commonly used windows are reported with the parameters exploited in this paper) [5].

The frequency index n is related to the frequency index h in (1)-(2) by $n \times \Delta f = f_h$, where $\Delta f = f_s/N_s$ is the DFT frequency resolution.

TABLE I
SOME FIGURES OF MERIT OF THREE WIDELY USED WINDOWS

Window	NPSG	ENBW
Rectangular	1	1
Hann	0.50	1.50
Minimum 4-term Blackman-Harris	0.36	2

Under non-coherent sampling conditions (i.e., when the number of acquired waveform periods is not an integer number), the relation $n \times \Delta f = f_h$ is intended as an approximate relation where n is the index such that $n \times \Delta f$ is the discrete frequency closest to f_h.

In this paper, according to [6], synchronization between sampling and the fundamental frequency component is assumed.

Therefore, frequency interpolation is not implemented for fundamental and harmonic components. For the same reason, the prescribed window in [6] is the rectangular window. In this paper, further kinds of windows are considered since in some cases spectral leakage from non-harmonic components could be significant if the simple rectangular window is used. The estimates of the active power are derived from (5)-(6) as:

$$\begin{gathered}\hat{P}_h = \left|\hat{V}_h\right|\left|\hat{I}_h\right| \cos\left(arg\hat{V}_h - arg\hat{I}_h\right) \\ h = 1, \dots, N \quad f_h \cong n \times \Delta f\end{gathered} \tag{7}$$

It is worth noticing that each of the RVs $\{\hat{P}_h\}_{h=1}^{N}$ defined by the transformation (7) is given as a function of four RVs $\left\{\left|\hat{V}_h\right|, \left|\hat{I}_h\right|, arg\hat{V}_h, arg\hat{I}_h\right\}$ for which statistical uncorrelation cannot be assumed. Indeed, it is well known that both $\left|\hat{V}_h\right|$ and $arg\hat{V}_h$ are obtained by combining the real and the imaginary parts of the relevant DFT coefficient $\hat{V}_h$, and the same is true for $\left|\hat{I}_h\right|$ and $arg\hat{I}_h$ with respect to the DFT coefficient $\hat{I}_h$.

It follows that the analytical derivation of the statistical properties of the RVs $\{\hat{P}_h\}_{h=1}^{N}$ given in the form (7) cannot be straightforward. In the next Section an alternative form for (7) will be provided, such that the statistical characterization of active power can be analytically derived through a straightforward approach.

III. Derivation of the Characteristic Function

In this Section, for the sake of simplicity, the frequency index h in (7) will be dropped since the proposed approach holds for each specific frequency f_h.

By using a well-known trigonometric identity, the active power (7) can be rewritten as

$$\begin{gathered}\hat{P} = \left|\hat{V}\right| cos\left(arg\hat{V}\right)\left|\hat{I}\right| cos\left(arg\hat{I}\right) + \\ +\left|\hat{V}\right| sin\left(arg\hat{V}\right)\left|\hat{I}\right| sin\left(arg\hat{I}\right) = \\ = \Re\{\hat{V}\}\Re\{\hat{I}\} + \Im\{\hat{V}\}\Im\{\hat{I}\}\end{gathered} \tag{8}$$

where the real ($\Re$) and the imaginary ($\Im$) parts of $\hat{V}$ and $\hat{I}$ have been put into evidence. By adopting a simpler notation (8) can be rewritten:

$$\hat{P} = \Re_V \Re_I + \Im_V \Im_I \tag{9}$$

In the literature it has been shown that each of the real and the imaginary parts of a DFT coefficient of a noisy waveform can be treated as Gaussian uncorrelated RVs, with mean value μ equal to the noise-free mean value (i.e., unbiased RVs), and variance given by [2], [5], [11], [16]-[17]:

$$\sigma^2 = \frac{1}{N_s}\sigma_n^2 ENBW \tag{10}$$

where σ_n^2 is the variance of the additive input noise, and ENBW is the Equivalent Noise Bandwidth of the selected time window.

Therefore, the RVs in (9) can be denoted as Gaussian RVs:

$$\Re_V \sim \mathcal{N}\left(\mu_{\Re_V}, \sigma_V^2\right), \qquad \Im_V \sim \mathcal{N}\left(\mu_{\Im_V}, \sigma_V^2\right) \tag{11}$$

$$\Re_I \sim \mathcal{N}\left(\mu_{\Re_I}, \sigma_I^2\right), \qquad \Im_I \sim \mathcal{N}\left(\mu_{\Im_I}, \sigma_I^2\right) \tag{12}$$

where the mean values are the noise-free values of DFT coefficients (possibly distorted by the contribution of the window in case of non-coherent sampling), and:

$$\sigma_V^2 = \frac{1}{N_s}\sigma_{n_v}^2 ENBW_V \tag{13}$$

$$\sigma_I^2 = \frac{1}{N_s}\sigma_{n_i}^2 ENBW_I \tag{14}$$

In (13) and (14) it has been taken into account that different windows with different ENBW can be used for the voltage and the current waveforms.

The expression obtained in (9) allows a straightforward derivation of the characteristic function of the active power.

In fact, the active power in (9) is written as the sum of two terms, where each term is the product of two uncorrelated Gaussian RVs. The characteristic function of the product of two Gaussian RVs is available in the technical literature [19].

Moreover, it is well-known that the characteristic function of the sum of two independent RVs is given by the product of the two characteristic functions [20].

The two elemental characteristic functions of the RVs in (9) are given by:

$$\begin{gathered}\Phi_{\Re_V \Re_I}(\omega) = \frac{1}{\sqrt{1 + (\sigma_V \sigma_I \omega)^2}} \cdot \\ \cdot \exp\left(-\frac{\begin{matrix}\omega^2\left(\sigma_I^2 \mu_{\Re_V}^2 + \sigma_V^2 \mu_{\Re_I}^2\right) + \\ -j2\omega\mu_{\Re_V}\mu_{\Re_I}\end{matrix}}{2(1 + (\sigma_V \sigma_I \omega)^2)}\right)\end{gathered} \tag{15}$$

$$\Phi_{\Im_V\Im_I}(\omega) = \frac{1}{\sqrt{1+(\sigma_V\sigma_I\omega)^2}} \cdot \cdot exp\left(-\frac{\omega^2\left(\sigma_I^2\mu_{\Im_V}^2 + \sigma_V^2\mu_{\Im_I}^2\right) - j2\omega\mu_{\Im_V}\mu_{\Im_I}}{2(1+(\sigma_V\sigma_I\omega)^2)}\right) \quad (16)$$

where $j = \sqrt{-1}$.

As mentioned above, the characteristic function of the RV (7) is given by the product of (15) and (16):

$$\Phi_{\hat{P}}(\omega) = \Phi_{\Re_V\Re_I}(\omega)\Phi_{\Im_V\Im_I}(\omega) = = \frac{1}{1+(\sigma_V\sigma_I\omega)^2} \cdot \cdot exp\left(-\frac{\omega^2(\sigma_I^2V^2 + \sigma_V^2I^2) - j2\omega P}{2(1+(\sigma_V\sigma_I\omega)^2)}\right) \quad (17)$$

where:

$$V^2 = \mu_{\Re_V}^2 + \mu_{\Im_V}^2 \quad (18)$$

$$I^2 = \mu_{\Re_I}^2 + \mu_{\Im_I}^2 \quad (19)$$

$$P = VIcos(\varphi - \vartheta) = \mu_{\Re_V}\mu_{\Re_I} + \mu_{\Im_V}\mu_{\Im_I} \quad (20)$$

are the unbiased rms squared voltage, rms squared current, and active power.

III.1 Fundamental Active Power

The characteristic function of the fundamental active power defined in (3) is given by (17) where the quantities (18)-(20) refer to the fundamental component:

$$\Phi_{\hat{P}_1}(\omega) = \frac{1}{1+(\sigma_V\sigma_I\omega)^2} \cdot \cdot exp\left(-\frac{\omega^2(\sigma_I^2V_1^2 + \sigma_V^2I_1^2) - j2\omega P_1}{2(1+(\sigma_V\sigma_I\omega)^2)}\right) \quad (21)$$

III.2 Harmonic Active Power

As far as the harmonic active power (4) is considered, by taking into account that the characteristic function of the sum of independent RVs is given by the product of the elemental characteristic functions we obtain:

$$\Phi_{\hat{P}_H}(\omega) = \prod_{h\neq 1}\Phi_{\hat{P}_h}(\omega) = = \frac{1}{[1+(\sigma_V\sigma_I\omega)^2]^{N_H}} \cdot \cdot exp\left(-\frac{\omega^2(\sigma_I^2V_H^2 + \sigma_V^2I_H^2) - j2\omega P_H}{2(1+(\sigma_V\sigma_I\omega)^2)}\right) \quad (22)$$

where [7]:

$$V_H^2 = \sum_{h\neq 1} V_h^2 \quad (23)$$

$$I_H^2 = \sum_{h\neq 1} I_h^2 \quad (24)$$

and N_H is the number of harmonic components in (23) and (24).

III.3. Extension to Polyphase Active-Power Measurement

Extension of (21) and (22) to electrical systems consisting in n wires is straightforward. In such cases, in fact, the total active power is given by the sum of n–1 single-phase power measurements by assuming one wire as reference.

The estimate of the total active power is therefore given by the sum of n–1 terms of the same kind as (9). Statistical independence of each of the n–1 terms results in a total characteristic function given by the product of n–1 terms of the same kind as (21) for the fundamental active power, and n–1 terms of the same kind as (22) for the harmonic active power.

IV. Statistical Moments

Statistical moments of fundamental and harmonic active power can be obtained from the characteristic functions derived in Section III.

The approach is based on the so-called moment-generating function which is related to the characteristic function by the variable substitution $s = j\omega$[20].

IV.1 Fundamental Active Power

From the characteristic function (21) the following moment-generating function can be derived:

$$M_{\hat{P}_1}(s) = \frac{1}{1-(\sigma_V\sigma_I s)^2} \cdot \cdot exp\left(\frac{s^2(\sigma_I^2V_1^2 + \sigma_V^2I_1^2) + 2sP_1}{2(1-(\sigma_V\sigma_I s)^2)}\right) \quad (25)$$

It is well-known from the moment theorem that the n-th derivative of (25) at the origin provides the n-th statistical moment of $\hat{P}$.

In particular, the first and second moments are given by:

$$M'_{\hat{P}_1}(0) = m_1 = P_1 \quad (26)$$

$$M''_{\hat{P}_1}(0) = m_2 = \sigma_I^2V_1^2 + \sigma_V^2I_1^2 + 2\sigma_V^2\sigma_I^2 + P_1^2 \quad (27)$$

from which the mean value and the variance can be readily derived:

$$\mu_{\hat{P}_1} = m_1 = P_1 \quad (28)$$

$$\sigma_{\hat{P}_1}^2 = m_2 - m_1^2 = \sigma_I^2V_1^2 + \sigma_V^2I_1^2 + 2\sigma_V^2\sigma_I^2 \quad (29)$$

It can be observed that the mean value (28) is unbiased.

Moreover, in (29) the first two terms take into account the magnitude of voltage and current spectral lines, whereas the third term is related only to noise.

By taking into account (13) and (14), the variance (29) can be written as explicit function of the number of samples N_s, of the selected time window with parameter *ENBW*, and of the additive noise variance σ_n^2:

$$\sigma_{\hat{P}_1}^2 = \frac{ENBW_I}{N_s}\sigma_{n_i}^2 V_1^2 + \frac{ENBW_V}{N_s}\sigma_{n_v}^2 I_1^2 + \\ +2\frac{ENBW_V ENBW_I}{N_s^2}\sigma_{n_v}^2\sigma_{n_i}^2 \tag{30}$$

By defining the voltage and current signal-to-noise-ratios:

$$SNR_{V_1} = \frac{V_1^2}{\sigma_{n_v}^2} \tag{31}$$

$$SNR_{I_1} = \frac{I_1^2}{\sigma_{n_i}^2} \tag{32}$$

the following expression for the standard deviation corresponding to (30) can be derived:

$$\sigma_{\hat{P}_1} = \sigma_{n_v}\sigma_{n_v}\sqrt{\frac{ENBW_I}{N_s}SNR_{V_1} + \frac{ENBW_V}{N_s}SNR_{I_1} + \\ +2\frac{ENBW_V ENBW_I}{N_s^2}} \tag{33}$$

Notice that (33) is slightly different from the result obtained in [2] by means of a different approach developed in the time domain.

Moreover, the approach presented in this paper, based on the characteristic function, allows straightforward calculation of higher order moments such as skewness and kurtosis [20].

IV.2. Harmonic Active Power

Statistical moments of the harmonic active power can be derived by applying to the characteristic function (22) the same approach presented in the previous subsection.

It can be easily shown that the mean value is still unbiased, i.e.:

$$\mu_{\hat{P}_H} = P_H \tag{34}$$

whereas the standard deviation is given by:

$$\sigma_{\hat{P}_H} = \\ = \sigma_{n_v}\sigma_{n_v}\sqrt{\frac{ENBW_I}{N_s}SNR_{V_H} + \frac{ENBW_V}{N_s}SNR_{I_H} + \\ +2N_H\frac{ENBW_V ENBW_I}{N_s^2}} \tag{35}$$

where:

$$SNR_{V_H} = \frac{V_H^2}{\sigma_{n_v}^2} \tag{36}$$

$$SNR_{I_H} = \frac{I_H^2}{\sigma_{n_i}^2} \tag{37}$$

V. Probability Density Function

The characteristic function of a RV is defined as the Fourier transform of the PDF [20]. Therefore, the PDF of fundamental and harmonic active power can be recovered from the characteristic functions (21) and (22) by means of the inversion formula:

$$f_{\hat{P}}(\hat{P}) = \frac{1}{2\pi}\int_{-\infty}^{\infty}\Phi_{\hat{P}}(\omega)e^{-j\omega\hat{P}}d\omega \tag{38}$$

The integral (38) can be easily evaluated numerically through standard methods. It is useful, however, to identify a finite integration interval to speed up the numerical process. To this aim, it can be readily recognized that the function $|\Phi_{\hat{P}}(\omega)|$ is equal to 1 for $\omega = 0$, whereas:

$$|\Phi_{\hat{P}}(\omega)| \sim \frac{1}{(\sigma_V\sigma_I\omega)^{2N_H}} \text{ when } \omega \to \pm\infty \tag{39}$$

Notice that $N_H = 1$ for the fundamental active power.

Therefore, reasonable integration limits in (39) can be defined by imposing

$$\frac{1}{(\sigma_V\sigma_I\omega)^{2N_H}} < \frac{1}{100} \tag{40}$$

leading to:

$$\omega_{lim} = \frac{10^{\frac{1}{N_H}}}{\sigma_V\sigma_I} \tag{41}$$

Thus the PDF can be recovered from:

$$f_{\hat{P}}(\hat{P}) \cong \frac{1}{2\pi}\int_{-\omega_{lim}}^{\omega_{lim}}\Phi_{\hat{P}}(\omega)e^{-j\omega\hat{P}}d\omega \tag{42}$$

where the range for the RV $\hat{P}$ can be roughly considered $\pm 3\sigma_{\hat{P}}$ centered on the mean value (28) or (34).

VI. Numerical Validation

The analytical results derived in the previous Sections were validated by resorting to numerical simulation of the whole process of active power measurement. Voltage and current waveforms consisting of the 60-Hz fundamental component and the first four odd harmonics were assumed (see Table II) according to the example reported in Annex A of [7].

TABLE II
HARMONIC CONTENT OF THE WAVEFORMS
FOR NUMERICAL VALIDATION

h	*f* (Hz)	$V_h\angle\varphi_h$ (V)	$I_h\angle\vartheta_h$ (A)	$P_h=V_hI_h\cos(\varphi_h-\vartheta_h)$ (W)
1	60	70.71 ∠-7.2	70.71 ∠-42.4	4085.72
3	180	5.02 ∠-76.0	19.09 ∠18.3	-7.18671
5	300	3.18 ∠-114.0	7.64 ∠-15.8	-3.46588
7	420	2.33 ∠-142.0	3.68 ∠-43.2	-1.31261
9	540	1.13 ∠-165.0	1.41 ∠-69.0	-0.16724

In this case for the voltage waveform we have $V_1 = 70.71\,V$ and $V_H = 6.48\,V$ according to (23), whereas for the current waveform we have $I_1 = 70.71\,A$ and $I_H = 20.94\,A$ according to (24). The fundamental active power is $P_1 = 4085.72\,W$ whereas the harmonic active power is $P_H = -12.13\,W$ according to (4).

Gaussian zero-mean independent noise was added to both voltage and current waveforms by selectingσ_{n_v} and σ_{n_i} according to the *SNR* values defined in (31)-(32) in case of fundamental active power evaluation, and (36)-(37) in case of harmonic active power evaluation. For the sake of simplicity, in the following simulations equal values for voltage and current SNR were selected, therefore we assume $SNR_V = SNR_I$, and such common value will be denoted as *SNR*. Simulations were performed by digitizing exactly 12 cycles of the fundamental frequency.

Thus, coherent sampling was implemented (i.e., synchronized measurements as recommended in [6]) such that interpolation algorithms against picket fence effects are not needed

The first set of simulations (Figs. 1-2) was addressed to validate the standard deviation (35) for the harmonic active power P_H. In Fig. 1 the standard deviation of P_H is shown as a function of *SNR* (analytical results (35) represented in solid lines). Numerical estimates of harmonic active power standard deviation (cross markers) have been obtained by 10^4 repeated evaluations of (4) through the relevant DFT spectral lines (5)-(6) for each *SNR* value.

Simulations were performed with a measurement window with length $N_S = 2^{10} = 1024$ samples. Three different windows have been used (see Table I) against spectral leakage from possible non-harmonic components. In any case, for all the simulations presented in this Section the same window was used for the voltage and current waveforms. Therefore, $ENBW_V = ENBW_I = ENBW$ was assumed.

According to (35), a window with larger *ENBW* results in a larger standard deviation. This is confirmed in Fig. 1, where the maximum values of the standard deviation have been obtained with the Blackman-Harris window having $ENBW = 2$, whereas the minimum standard deviation has been obtained with the rectangular window having $ENBW = 1$. Intermediate values have been obtained with the Hann window having $ENBW = 1.5$. In Fig. 2, the standard deviation (35) for the harmonic active power was validated with respect to the number of samples N_S.

Simulations were performed with three different number of samples, i.e., 256, 1024, and 4096.

The selected window was the Hann window. As it was expected from (35), the standard deviation increases with decreasing number of samples.

The second set of simulations (Figs. 3-6) was addressed to validate the PDF of both the fundamental and the harmonic active power.

Fig. 3 refers to the fundamental active power and compares (42) (evaluated for the characteristic function (21)) with numerical results obtained by a repeated run analysis, for the three numbers of samples already considered in Fig. 2. The window is the rectangular one since coherent sampling is assumed with respect to the fundamental component.

Additive noise is such that $SNR = 10^4$. Behavior of the curves is in agreement with (33). In fact, by increasing the number of samples the standard deviation of fundamental active power decreases and therefore a more peaked PDF is expected. Fig. 4 reports the PDFs of the harmonic active power in the same conditions defined for Fig. 3 and assuming $SNR = 10^2$. Analytical PDFs are obtained from (42) and (22). The same remarks reported above for Fig. 3 can be done with respect to the impact of the number of samples on the standard deviation (35).

In Fig. 5 the PDF (42) for the harmonic active power is validated against different windows. The number of samples is 1024 and the $SNR = 10^2$. According to (35), windows with larger *ENBW* result in larger standard deviation of harmonic active power and then PDF with lower peak.

In Fig. 6 three different *SNR* were set for the evaluation of the PDF of harmonic active power. The number of samples is 1024 and a rectangular window was applied. By increasing the *SNR* the PDF spread decreases due to lower noise contribution.

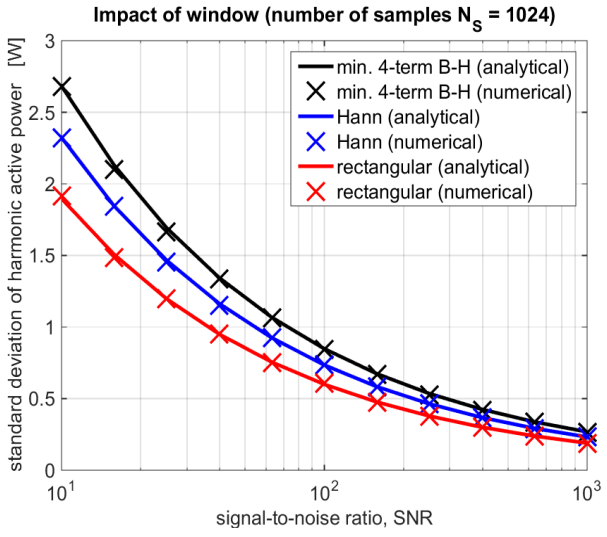

Fig. 1. Standard deviation of the harmonic active power as a function of the signal-to-noise ratio of voltage and current waveforms. Comparison between analytical result (35) (solid lines) and numerical results (markers) for different windows and 1024 samples

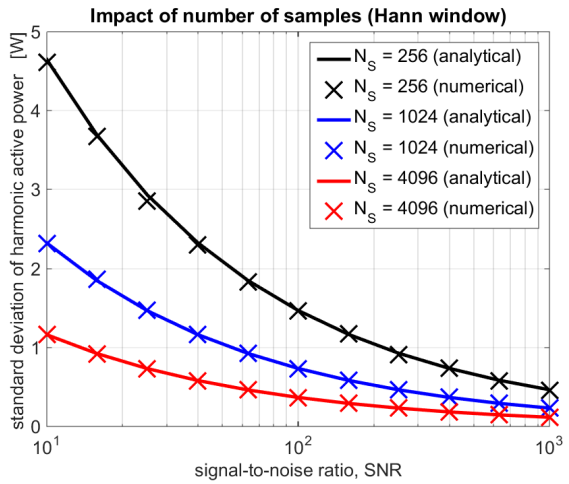

Fig. 2. Standard deviation of the harmonic active power as a function of the signal-to-noise ratio of voltage and current waveforms. Comparison between analytical result (35) (solid lines) and numerical results (markers) for different number of samples, and Hann window

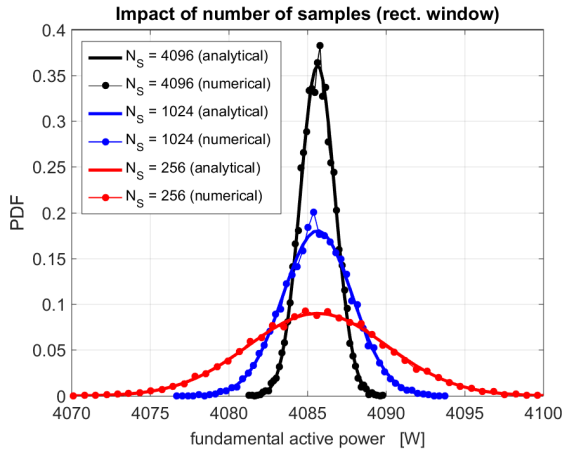

Fig. 3. Probability density function of the fundamental active power for different numbers of samples. Comparison between analytical results (42) and (21) (solid lines) with numerical results (markers) by assuming $SNR=10^4$ and rectangular window

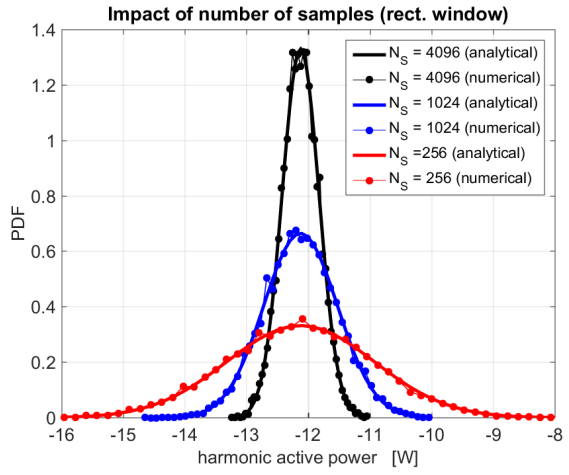

Fig. 4. Probability density function of the harmonic active power for different numbers of samples. Comparison between analytical results (42) and (22) (solid lines) with numerical results (markers) by assuming $SNR=10^2$ and rectangular window

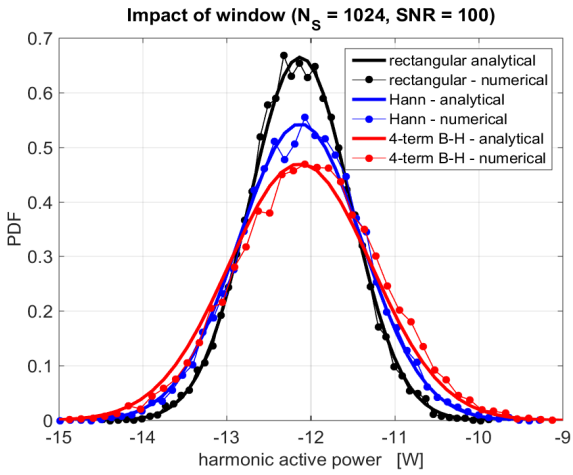

Fig. 5. Probability density function of the harmonic active power for different windows. Comparison between analytical results (42) and (22) (solid lines) with numerical results (markers) by assuming $SNR=10^2$ and 1024 samples

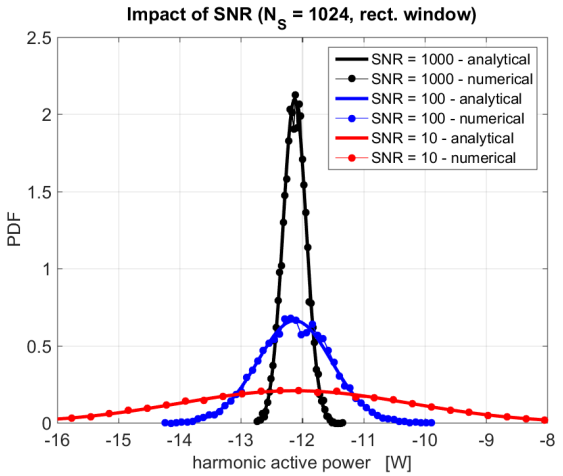

Fig. 6. Probability density function of the harmonic active power for different *SNR* values. Comparison between analytical results (42) and (22) (solid lines) with numerical results (markers) by assuming rectangular window and 1024 samples

VII. Conclusion

Analytical expressions for the standard deviation and the PDF of fundamental and harmonic active power from noisy measurements have been derived as functions of the sampling parameters (i.e., the number of samples and the window) and of the voltage/current waveforms parameters. Although the PDF has been derived in implicit (integral) form, its numerical evaluation was effectively performed through standard discretization of the Fourier integral. Therefore, such integral expression can be advantageously used to predict the impact of the relevant parameters on the probabilistic properties of the estimated power. Of course, the proposed approach is useful when additive noise plays a significant role, i.e., for harmonic active power in the case of low SNR.

This can be the case of the modern electrical power systems where power quality issues require more and more detailed evaluations.

References

[1] C. Gherasim, J. Van den Keybus, J. Driesen, and R. Belmans, DSP Implementation of Power Measurements According to the IEEE Trial-Use Standard 1459,*IEEE Trans. on Instrum. Meas*., *vol. 53*, no. 4, Aug. 2004, pp. 1086-1092.

[2] P. Carbone and D. Petri,Average power estimation under nonsinusoidal conditions,*IEEE Trans. on Instrum. Meas*., *vol. 49*, no. 2, April 2000, pp. 333-336.

[3] A. Cataliotti, V. Cosentino, S. Nuccio, A time domain approach for IEEE Std 1459-2000 powers measurement in distorted and unbalanced power systems, in *Proc. of the IEEE IMTC 2004*, Como, Italy, 18-20 May 2004, pp. 1388-1393.

[4] J. Arrillaga and N. R. Watson, *Power system harmonics* (John Wiley & Sons Ltd, 2003).

[5] Bellan, D., Statistical characterization of harmonic emissions in power supply systems, (2014) *International Review of Electrical Engineering (IREE),* 9 (4), pp. 803-810.

[6] IEC 61000-4-7, *Electromagnetic compatibility (EMC) – Part 4-7: Testing and measurement techniques – General guide on harmonics and interharmonics measurements and instrumentation, for power supply systems and equipment connected thereto*(IEC, 2002).

[7] IEEE Std 1459™, *IEEE Standard definitions for the measurement of electric power quantities under sinusoidal, nonsinusoidal, balanced or unbalanced conditions* (IEEE, 2010).

[8] Ai, Y., Zheng, J., Analysis on affecting factors of harmonic power flow, (2014) *International Review of Electrical Engineering (IREE),* 9 (3), pp. 585-591.

[9] Ahmad, N.H.T., Abdullah, A.R., Abidullah, N.A., Jopri, M.H., Analysis of power quality disturbances using spectrogram and S-Transform, (2014) *International Review of Electrical Engineering (IREE),* 9 (3), pp. 611-619.

[10] Chun, G., Zhu, Q., Recognition of multiple power quality disturbances using KNN-Bayesian, (2014) *International Review of Electrical Engineering (IREE),* 9 (1), pp. 109-112.

[11] D. Agrez, Power measurement in the non-coherent sampling, *Measurement, vol. 41*, 2008, pp. 230-235.

[12] D. Bellan, A. Brandolini, and A. Gandelli, Quantization theory in electrical and electronic measurements, in *Proc. 1995 IEEE Instrumentation and Measurement Technology Conference*, Waltham, MA, USA, April 23-26, 1995, pp. 494-499.

[13] D. Bellan, A. Brandolini, and A. Gandelli, ADC nonlinearities and harmonic distortion in FFT test, in *Proc. 1998 IEEE Instrumentation and Measurement Technology Conference*, St. Paul, MN, USA, May 18-21, 1998, pp. 1233-1238.

[14] D. Bellan, Model for the spectral effects of ADC nonlinearity, *Measurement*, *vol. 26*, no. 2, 2000, pp. 65-76.

[15] D. Bellan, Frequency instability and additive noise effects on digital power measurements under nonsinusoidal conditions, in *Proc. of 2014 6th IEEE Power India International Conference*, Delhi, India, Dec. 5-7, 2014, pp. 1-5.

[16] O. M. Solomon, The use of DFT windows in signal-to-noise ratio and harmonic distortion computations,*IEEE Trans. Instrum. Meas*., *vol. 43*, April 1994,pp. 194-199.

[17] D. Bellan, A. Gaggelli, and S. A. Pignari, Noise Effects in Time-Domain Systems Involving Three-Axial Field Probes for the Measurement of Nonstationary Radiated Emissions, *IEEE Trans. on Electromagn. Compat.*, vol. 51, no. 2, May 2009, pp. 192-203.

[18] F. J. Harris, On the use of windows for harmonic analysis with the discrete Fourier transform,*Proc. of the IEEE*, vol. 66, 1978, pp. 51-83.

[19] M. K. Simon, *Probability Distributions Involving Gaussian Random Variables* (Springer, 2002).

[20] A. Papoulis, *Probability, random variables, and stochastic processes* (3rd ed., McGraw-Hill, 1991).